

Three-photon excited fluorescence imaging of unstained tissue using a GRIN lens endoscope

David M. Huland,^{1,3,*} Kriti Charan,^{1,3} Dimitre G. Ouzounov,¹
Jason S. Jones,² Nozomi Nishimura,² and Chris Xu¹

¹School of Applied and Engineering Physics, Cornell University, 146 Clark Hall, Ithaca, NY 14853, USA

²Department of Biomedical Engineering, Cornell University, B57 Weill Hall, Ithaca, NY 14853, USA

³These authors contributed equally to this work

*dmh56@cornell.edu

Abstract: We present a compact and portable three-photon gradient index (GRIN) lens endoscope system suitable for imaging of unstained tissues, potentially deep within the body, using a GRIN lens system of 1 mm diameter and 8 cm length. The lateral and axial resolution in water is 1.0 μm and 9.5 μm , respectively. The ~ 200 μm diameter field of view is imaged at 2 frames/s using a fiber-based excitation source at 1040 nm. *Ex vivo* imaging is demonstrated with unstained mouse lung at 5.9 mW average power. These results demonstrate the feasibility of three-photon GRIN lens endoscopy for optical biopsy.

©2013 Optical Society of America

OCIS codes: (170.2150) Endoscopic imaging; (180.4315) Nonlinear microscopy; (110.2760) Gradient-index lenses.

References and links

1. W. Denk, J. H. Strickler, and W. W. Webb, "Two-photon laser scanning fluorescence microscopy," *Science* **248**(4951), 73–76 (1990).
2. L. Fu, A. Jain, C. Cranfield, H. Xie, and M. Gu, "Three-dimensional nonlinear optical endoscopy," *J. Biomed. Opt.* **12**(4), 040501 (2007).
3. M. T. Myaing, D. J. MacDonald, and X. Li, "Fiber-optic scanning two-photon fluorescence endoscope," *Opt. Lett.* **31**(8), 1076–1078 (2006).
4. D. R. Rivera, C. M. Brown, D. G. Ouzounov, I. Pavlova, D. Kobat, W. W. Webb, and C. Xu, "Compact and flexible raster scanning multiphoton endoscope capable of imaging unstained tissue," *Proc. Natl. Acad. Sci. U.S.A.* **108**(43), 17598–17603 (2011).
5. S. Tang, W. Jung, D. McCormick, T. Xie, J. Su, Y.-C. Ahn, B. J. Tromberg, and Z. Chen, "Design and implementation of fiber-based multiphoton endoscopy with microelectromechanical systems scanning," *J. Biomed. Opt.* **14**(3), 034005 (2009).
6. Y. Wu, Y. Leng, J. Xi, and X. Li, "Scanning all-fiber-optic endomicroscopy system for 3D nonlinear optical imaging of biological tissues," *Opt. Express* **17**(10), 7907–7915 (2009).
7. E. J. Seibel and Q. Y. J. Smithwick, "Unique features of optical scanning, single fiber endoscopy," *Lasers Surg. Med.* **30**(3), 177–183 (2002).
8. D. R. Rivera, C. M. Brown, D. G. Ouzounov, W. W. Webb, and C. Xu, "Use of a lensed fiber for a large-field-of-view, high-resolution, fiber-scanning microendoscope," *Opt. Lett.* **37**(5), 881–883 (2012).
9. D. R. Rivera, C. M. Brown, D. G. Ouzounov, W. W. Webb, and C. Xu, "Multifocal multiphoton endoscope," *Opt. Lett.* **37**(8), 1349–1351 (2012).
10. C. M. Brown, D. R. Rivera, I. Pavlova, D. G. Ouzounov, W. O. Williams, S. Mohanan, W. W. Webb, and C. Xu, "*In vivo* imaging of unstained tissues using a compact and flexible multiphoton microendoscope," *J. Biomed. Opt.* **17**(4), 040505 (2012).
11. D. M. Huland, C. M. Brown, S. S. Howard, D. G. Ouzounov, I. Pavlova, K. Wang, D. R. Rivera, W. W. Webb, and C. Xu, "*In vivo* imaging of unstained tissues using long gradient index lens multiphoton endoscopic systems," *Biomed. Opt. Express* **3**(5), 1077–1085 (2012).
12. D. Kobat, M. E. Durst, N. Nishimura, A. W. Wong, C. B. Schaffer, and C. Xu, "Deep tissue multiphoton microscopy using longer wavelength excitation," *Opt. Express* **17**(16), 13354–13364 (2009).
13. D. Kobat, N. G. Horton, and C. Xu, "*In vivo* two-photon microscopy to 1.6-mm depth in mouse cortex," *J. Biomed. Opt.* **16**(10), 106014 (2011).
14. L.-H. Chen, S.-W. Chu, C.-K. Sun, P.-C. Cheng, and B.-L. Lin, "Wavelength dependent damage in biological multi-photon confocal microscopy: A micro-spectroscopic comparison between femtosecond Ti:sapphire and Cr:forsterite laser," *Opt. Quantum Electron.* **34**(12), 1251–1266 (2002).
15. Y. Fu, H. Wang, R. Shi, and J.-X. Cheng, "Characterization of photodamage in coherent anti-Stokes Raman scattering microscopy," *Opt. Express* **14**(9), 3942–3951 (2006).

16. G. Liu, K. Kieu, F. W. Wise, and Z. Chen, "Multiphoton microscopy system with a compact fiber-based femtosecond-pulse laser and handheld probe," *J. Biophotonics* **4**(1-2), 34–39 (2011).
17. C. Xu, W. R. Zipfel, J. B. Shear, R. M. Williams, and W. W. Webb, "Multiphoton fluorescence excitation: new spectral windows for biological nonlinear microscopy," *Proc. Natl. Acad. Sci. U.S.A.* **93**(20), 10763–10768 (1996).
18. S. W. Hell, K. Bahlmann, M. Schrader, A. Soini, H. M. Malak, I. Gryczynski, and J. R. Lakowicz, "Three-photon excitation in fluorescence microscopy," *J. Biomed. Opt.* **1**(1), 71–74 (1996).
19. D. L. Wokosin, V. E. Centonze, S. Crittenden, and J. White, "Three-photon excitation fluorescence imaging of biological specimens using an all-solid-state laser," *Bioimaging* **4**(3), 208–214 (1996).
20. W. R. Zipfel, R. M. Williams, R. Christie, A. Y. Nikitin, B. T. Hyman, and W. W. Webb, "Live tissue intrinsic emission microscopy using multiphoton-excited native fluorescence and second harmonic generation," *Proc. Natl. Acad. Sci. U.S.A.* **100**(12), 7075–7080 (2003).
21. S. Maiti, J. B. Shear, R. M. Williams, W. R. Zipfel, and W. W. Webb, "Measuring serotonin distribution in live cells with three-photon excitation," *Science* **275**(5299), 530–532 (1997).
22. N. G. Horton, K. Wang, D. Kobat, C. G. Clark, F. W. Wise, C. B. Schaffer, and C. Xu, "*In vivo* three-photon microscopy of subcortical structures within an intact mouse brain," *Nat. Photonics* **7**(3), 205–209 (2013).
23. J. G. Fujimoto, C. Pitris, S. A. Boppart, and M. E. Brezinski, "Optical coherence tomography: an emerging technology for biomedical imaging and optical biopsy," *Neoplasia* **2**(1-2), 9–25 (2000).
24. J. M. Squirrell, D. L. Wokosin, J. G. White, and B. D. Bavister, "Long-term two-photon fluorescence imaging of mammalian embryos without compromising viability," *Nat. Biotechnol.* **17**(8), 763–767 (1999).
25. D. G. Ouzounov, D. R. Rivera, C. M. Brown, W. W. Webb, and C. Xu, "Dual modality microendoscope with optical zoom capability," in *CLEO 2012*, San Jose, CA (Optical Society of America, 2012), postdeadline paper ATh5A.2.
26. C. J. Engelbrecht, R. S. Johnston, E. J. Seibel, and F. Helmchen, "Ultra-compact fiber-optic two-photon microscope for functional fluorescence imaging *in vivo*," *Opt. Express* **16**(8), 5556–5564 (2008).
27. P. Theer, M. T. Hasan, and W. Denk, "Two-photon imaging to a depth of 1000 μm in living brains by use of a Ti:Al₂O₃ regenerative amplifier," *Opt. Lett.* **28**(12), 1022–1024 (2003).
28. G. A. Sonn, S. N. Jones, T. V. Tarin, C. B. Du, K. E. Mach, K. C. Jensen, and J. C. Liao, "Optical biopsy of human bladder neoplasia with *in vivo* confocal laser endomicroscopy," *J. Urol.* **182**(4), 1299–1305 (2009).

1. Introduction

In vivo two-photon (2P) microscopy has become a valuable tool for the study of subsurface features in intact tissues and organs [1]. To be clinically useful, endoscopic 2P approaches are required. A number of different endoscopes and techniques have been demonstrated in the past [2–9], including *in vivo* imaging of unstained tissues [10,11].

Previous 2P endoscope demonstrations rely on the mode-locked Ti:S laser at 800 nm to excite intrinsic fluorescence. However, longer excitation wavelengths have been shown to provide several advantages. As a result of an increased scattering length in tissue for longer excitation sources, the imaging penetration depth can be increased significantly using longer excitation wavelengths [12,13]. There are also strong indications that using longer wavelengths could lead to diminished phototoxicity. For example, imaging with longer wavelength has been shown to reduce destructive plasma formation [14,15]. Furthermore, femtosecond pulsed excitation at 1030 to 1070 nm can be conveniently provided by robust, compact fiber based lasers, which will significantly reduce the cost and improve the clinical compatibility. Although fiber lasers at these wavelengths can be used for 2P imaging of red dyes [16], 2P excitation of intrinsic molecules such as nicotinamide adenine dinucleotide (NADH) and flavin adenine dinucleotide (FAD) is impractical using the fiber source due to their small 2P cross sections at the long wavelengths [17].

Three-photon (3P) microscopy was first demonstrated in the 1990s [17–19]. 3P excitation is an effective approach to extend the spectral range of the excitation source. For example, 3P intrinsic fluorescence microscopy has been performed with deep UV-excitable intrinsic fluorophores such as serotonin and melatonin [20,21]. Here we demonstrate a GRIN lens endoscope that is capable of imaging unstained mouse lung tissues using 3P excitation by a fiber laser at 1040 nm. To the best of our knowledge, this is the first demonstration of 3P imaging of unstained tissues through a compact and portable system with potential for endoscopic tissue diagnosis.

2. Endoscope design and characterization

The compact and portable GRIN lens endoscope is shown in Fig. 1, which was described in our previous work for 2P excitation of intrinsic fluorescence using a mode-locked Ti:S laser at 800 nm [11]. This system weighs less than 2lbs and was used successfully for *in vivo* 2P imaging in rats. For 3P endoscopic imaging, we used a longer wavelength, fiber laser source. (IMRA μ Jewel laser, 1040 nm wavelength and 1 MHz repetition rate). The optical components such as scan mirrors, scan lenses, objective and GRIN lens system are compatible with this new excitation source. For example, we found that the transmission of the GRIN lens is $\sim 80\%$ at 1040 nm, which is adequate for our applications. Modifications were made in the pulse delivery. The excitation light is delivered to the endoscope via a 1.6 m long hollow-core photonic band-gap fiber (HC-1060-2, NKT Photonics). A half-wave plate (WPH05M-1053, Thorlabs Inc.) was used to align the polarization of the excitation light with the polarization axis of the fiber. An aspheric lens on the portable GRIN lens endoscope collimates the excitation light to a beam about 2 mm in diameter. A small aperture (3 mm), galvanometer scanning mirror system (6210H, Cambridge Technology) allows for a fast imaging rate (up to 4 frames/s at 512 by 512 pixels). The beam is then expanded by two scan lenses 18 and 36 mm in focal length (respectively, LSM02-BB and LSM03-BB, Thorlabs Inc.) to underfill a 0.3 NA microscope objective (RMS10X-PF, Thorlabs Inc.) to achieve an effective focusing NA of ~ 0.1 . A polarizer was added between the scan lenses to eliminate any residual light in the orthogonal polarization. The microscope objective couples the excitation beam into the proximal side of the GRIN lens system. This 1 mm diameter system is composed of a 0.1 NA relay lens (1.75 pitch) and a 0.5 NA objective lens (<0.25 pitch), resulting in a total probe length of 8 cm. The fluorescence signal from the sample is epi-collected through the GRIN lenses and the microscope objective, and is reflected by a dichroic beam splitter (FF705-Di01, Semrock Inc.). After passing through one short pass filter (FF01-720/SP, Semrock Inc.), a notch dichroic (NFD01-532, Semrock Inc.) separates the signal into the second harmonic generation (SHG) and the autofluorescence channel. Another 520 nm bandpass filter (FF01-520/15, Semrock Inc.) is used to further minimize autofluorescence collection in the SHG channel. The housing of the GRIN lens endoscope is constructed from custom machined aluminum components using a milling machine with a fabrication tolerance of 0.001". Optical characterizations were conducted by moving the sample mounted on a 3D stage (MP-285, Sutter Instruments), allowing axial scanning of the sample while maintaining the GRIN lens endoscope system in a fixed position.

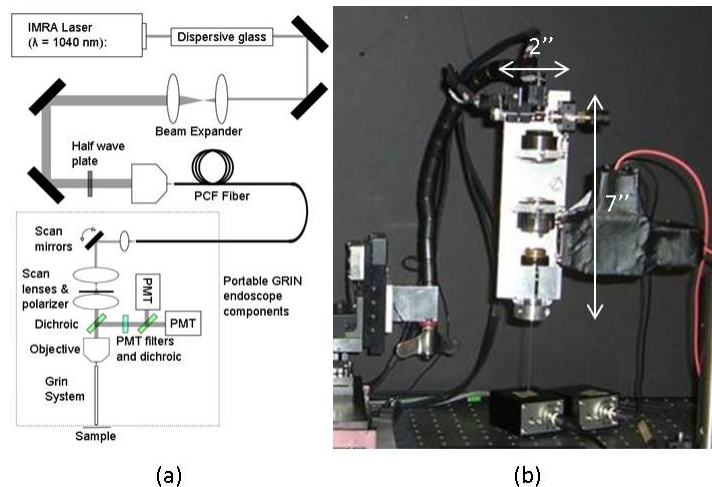


Fig. 1. Portable GRIN lens endoscope. (a) Optical setup and (b) Photograph of the GRIN lens based endoscope system. Total system length of the portable device is 10.6" (including GRIN lens system).

To compensate for the fiber's anomalous dispersion, the pulses were pre-chirped by using a long piece of SF11 glass (Schott). Second order interferometric autocorrelations were performed to optimize the dispersion compensation by measuring the pulse-width at the sample for different lengths of SF11 glass before the fiber. We found that 65 cm of SF11 glass produced the shortest pulse with an intensity autocorrelation full-width at half-maximum (FWHM) of 509 fs. The resulting autocorrelation traces are shown in Fig. 2.

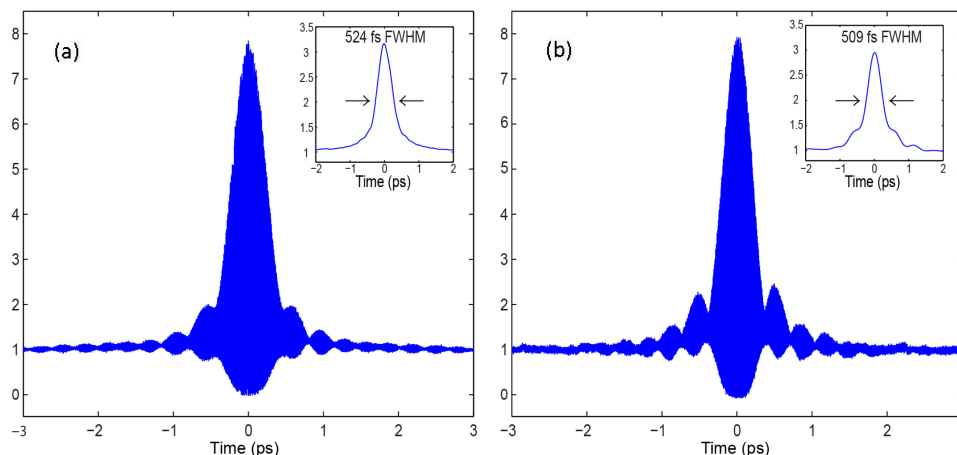


Fig. 2. Second order interferometric autocorrelation traces of the pulse. (a) Directly from the source, inset: the corresponding intensity autocorrelation with a pulse width of 524 fs, (b) at the sample (i.e., after dispersion compensation using 65 cm of SF11 glass, the hollow core fiber, the optical components, and the GRIN lens), inset: the corresponding intensity autocorrelation with a pulse width of 509 fs.

We imaged fluorescent beads (0.1 μm diameter, absorption peak 350 nm, emission peak 440 nm, Invitrogen) embedded in agarose gel and with water immersion to characterize the lateral and axial 3P resolution. The FWHM for the lateral and axial resolution is 1.0 μm and 9.5 μm , respectively (Fig. 3). To confirm 3P excitation, fluorescence signal was measured at 5 different excitation powers while the laser beam was fixed on a bead. Figure 3(c) shows that the fluorescence signal generated closely follows a cubic dependence on the excitation power. To demonstrate the capability of our device for imaging intrinsic fluorescence, we imaged unstained mouse lung tissue *ex vivo*. A 3 month old female, wild type mouse (Jackson Labs) was euthanized and a lung lobe was removed, embedded in agarose gel and plated on a standard glass microscope slide. The tissue was imaged within 1 hour of euthanasia using 5.9 mW at the sample and at a frame rate of 2 frames/s (512 by 512 pixels). Representative images are shown in Figs. 4(a)-4(c). We can identify the surface of the lung with strong SHG signal coming presumably from the pleura (Fig. 4(a)). Below that, we can identify individual circular alveoli Figs. 4(b)-4(c), showing that the images could potentially provide diagnostic information. To confirm 3P excitation, fluorescence photons of the autofluorescence channel were measured at 5 different excitation powers at the sample by photon counting while scanning the laser beam at a fixed area in the tissue. Figure 4(d) shows that the fluorescence signal generated from the unstained tissue closely follows a cubic dependence on the excitation power, confirming that the image contrast is indeed generated by 3P excitation of intrinsic fluorescence.

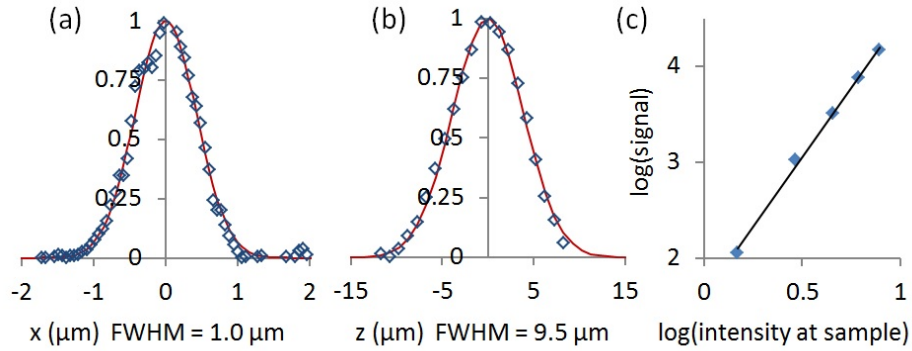


Fig. 3. Three-photon lateral and axial resolution of the GRIN lens endoscope system. (a) Lateral and (b) axial intensity line profile across a subresolution fluorescent bead (blue diamonds). The Gaussian fits are indicated by the red lines. (c) Log-log plot of fluorescence signal as a function of excitation power at the sample. The slope is 2.9, indicating that the signal is generated by 3P excitation. Data in (c) was acquired using an ultrafast fiber laser at 1030 nm (Satsuma, Amplitude Systems, 5.7 MHz repetition rate).

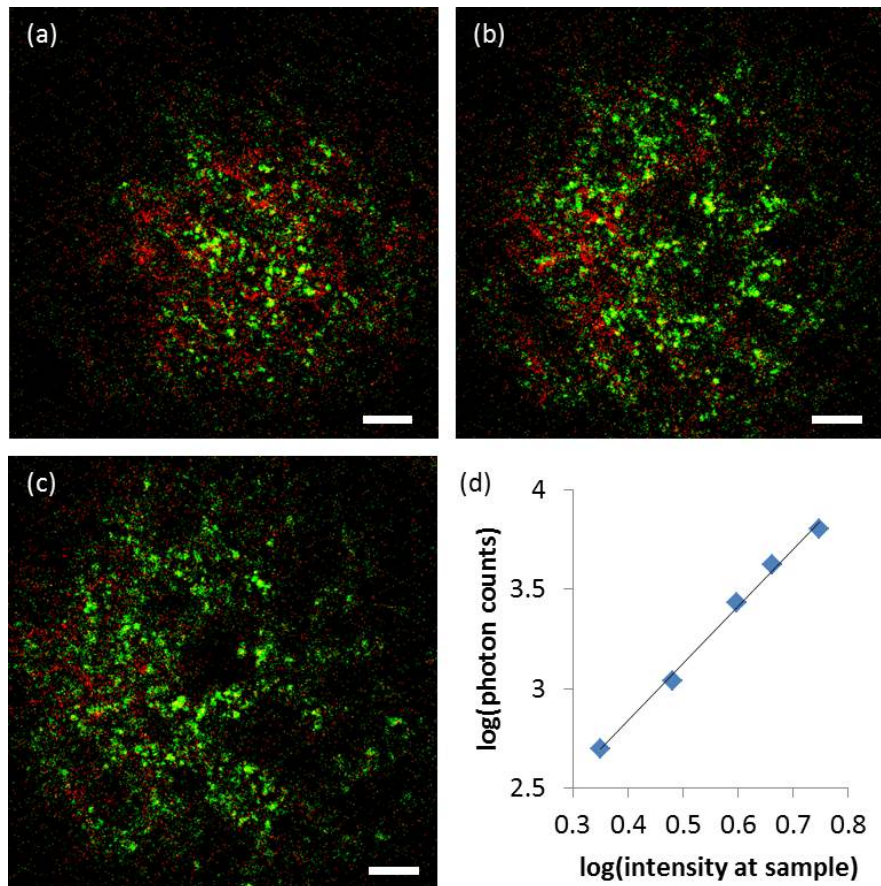


Fig. 4. Unaveraged image of *ex vivo* unstained mouse lung acquired at 2 frames/s. Green: 3P autofluorescence. Red: SHG. Scale bar is 20 μm. Images taken at (a) 20 μm, (b) 30 μm, and (c) 40 μm below the tissue surface. (d) Log-log plot of autofluorescence signal as a function of excitation power at the sample. The slope is 2.9, indicating that the signal is generated by 3P excitation.

3. Discussion

Our results demonstrated the feasibility of 3P imaging of intrinsic fluorescence in a GRIN lens endoscope. As compared to our previous 2P imaging results at 800 nm using the same device [11], the resolution of 3P imaging at 1040 nm degrades slightly, 1.0 μm lateral and 9.5 μm axial for 3P imaging vs. 0.85 μm lateral and 7.4 μm axial for 2P imaging. Since the GRIN lens system was originally designed for 800 nm excitation, the imaging performance at 1040 nm may be somewhat degraded. Nonetheless, our results showed that the spatial resolution is sufficient to provide diagnostic information.

There are several advantages for 3P endoscopy as compared to 2P endoscopy. The longer excitation wavelength and 3P excitation significantly improve the capability of tissue penetration [22], which is desirable for tissue diagnostics. 3P excitation allows the use of compact, convenient fiber femtosecond laser as the excitation source, which significantly reduces the cost and improves the clinical compatibility. Furthermore, the fiber laser at 1040 nm can excite intrinsic molecules (e.g., NADH, FAD) significantly closer to their 3P excitation peaks than 2P excitation at 800 nm [20]. While the pulse energy has increased in our demonstration as compared to our 2P endoscope, we found that the required average power for image generation is less than 6 mW, bringing multiphoton endoscopy to average power levels comparable to other optical diagnostic techniques such as confocal endoscopy and optical coherence tomography [23]. While the exact impact of pulse energy, duration, wavelength and average power on tissue damage needs to be investigated further, previous studies showed a lower phototoxicity at longer wavelengths [14,15,24]. We note that third harmonic generation (THG), which is much more ubiquitous than SHG, could potentially be added as another imaging contrast. Although THG imaging is not possible in our experiments because the transmission of the GRIN lens we used drops significantly below 370 nm, there is no fundamental limitation in making new lenses with high transmission at ~ 350 nm.

The main disadvantage of 3P endoscopy would be an increase in chromatic aberrations in the endoscope optics due to the larger difference between the excitation and signal wavelengths. The impact of this, however, can be reduced by carefully designing the optics for specific applications. Fiber delivery of the energetic femtosecond pulses for 3P excitation is another concern. The use of hollow core fibers, as shown in this paper, overcomes this difficulty. While hollow core fibers cannot effectively collect the fluorescence signal back through the excitation path, efficient signal collection through non-reciprocal optical path (e.g., using large core multimode fibers) has been demonstrated in the past [25,26]. Thus, 3P excitation can be implemented in a flexible endoscope with a small rigid tip.

It should be noted that although we used a fiber laser that is capable of producing average power up to 1 W (i.e., 1 μJ pulses), less than 6 mW (i.e., 6 nJ pulses) was used at the sample in our experiments. Compact, fiber based femtosecond oscillators producing >40 nJ pulse energy are commercially available. These sources are adequate for 3P excitation of intrinsic fluorophores assuming a reasonable system throughput of $\sim 25\%$. Furthermore, our frame rate (2 frames per second) was limited by the low repetition rate of the laser (1 MHz). Oscillators providing higher repetition rates (e.g., 3 MHz) and shorter pulses (e.g., 150 fs) can significantly increase the imaging acquisition rate without increasing the average excitation power, which will be valuable for overcoming motion artifacts for *in vivo* applications. Alternatively, the pixel clock of the image acquisition system could be synchronized to the laser pulses to maximize the frame rate [27]. For example, 3 MHz repetition rate can provide a maximum frame rate of ~ 12 frames/s at 512 pixels by 512 pixels per frame, which is adequate to overcome motion artifacts in *in vivo* imaging. Such a frame rate was shown to be adequate for *in vivo* imaging of Fluorescein stained human bladders using a confocal laser endoscope [28].

4. Conclusion

We have demonstrated the feasibility of 3P intrinsic fluorescence endoscopy using a GRIN lens endoscope and a fiber-based excitation source at 1040 nm. The compact and portable

device can acquire 3P intrinsic fluorescence and SHG images at a rate of 2 frames/s with a field-of-view of ~ 200 μm diameter with subcellular resolution. The presented *ex vivo* results of unstained mouse lung tissue show great promise for using 3P GRIN lens endoscopy for optical biopsy. The combination of longer wavelength and 3P excitation, together with the convenient fiber-based excitation source, may make 3P endoscopy a valuable alternative to the conventional 2P approach.

Acknowledgments

This research was made possible by National Institutes of Health/National Cancer Institute Grant Number R01-CA133148 and National Institutes of Health/National Institute of Biomedical Imaging and Bioengineering Grant Numbers R01EB014873 and R01-EB006736. We thank members of the Xu and Schaffer-Nishimura research groups for discussions and technical suggestions.